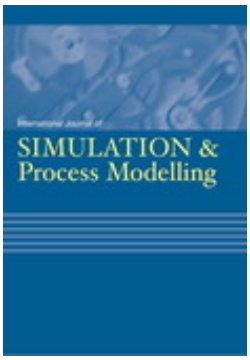

International Journal of Simulation and Process Modelling

ISSN online: 1740-2131 - ISSN print: 1740-2123
https://www.inderscience.com/ijspm

Tau protein transmission simulation modelling in Alzheimer's disease integrated with neuro-symbolic learning

Mengke Huo, Yajing Chen, Huiqin Wang

DOI: 10.1504/IJSPM.2026.10077519

Article History:

Received:	17 December 2025
Last revised:	28 January 2026
Accepted:	02 February 2026
Published online:	29 April 2026

Tau protein transmission simulation modelling in Alzheimer's disease integrated with neuro-symbolic learning

Mengke Huo, Yajing Chen and Huiqin Wang*

School of Health Medicine,
Zhengzhou Health College,
Zhengzhou, 450000, China
Email: huomengke2@zzsqmc.edu.cn
Email: cyj_2012@163.com
Email: wanghuiqin@zzsqmc.edu.cn
*Corresponding author

Abstract: Transneuronal propagation of Tau in Alzheimer's disease is a central mechanism of disease progression. We propose a computational framework incorporating neuro symbolic learning to model this multi-scale process. This model combines graph neural networks with symbolic rules encoding biological priors (e.g., prion-like propagation, metabolic activity promotion), and constructs a bridge from 'cognitive load theory' to 'computable pathological model'. Experiments based on the Alzheimer's disease neuroimaging initiative real dataset (n = 428) show that NSTP-Net has the root mean square error (0.135) significantly lower than the current advanced methods in predicting the Tau distribution over the next 18 months, and the performance improvement reaches 22% ($p < 0.001$). The model also had high accuracy in predicting Mild Cognitive Impairment to Alzheimer's disease conversion. This study provides an interpretable new tool for understanding the mechanism of Tau propagation and demonstrates important clinical potential for individualised prognosis prediction.

Keywords: Alzheimer's disease; Tau protein transmission; neuro symbolic learning; graph neural network; computational pathological model.

Reference to this paper should be made as follows: Huo, M., Chen, Y. and Wang, H. (2026) 'Tau protein transmission simulation modelling in Alzheimer's disease integrated with neuro-symbolic learning', *Int. J. Simulation and Process Modelling*, Vol. 23, No. 6, pp.1–12.

Biographical notes: Mengke Huo is a Lecturer at Zhengzhou Health College, China. She received her Bachelor's degree from Sanquan College of Xinxiang Medical College (2017) and Master's degree from Dali University (2020), China. Her research interests include pathophysiology, neurology, post-traumatic stress disorder, Alzheimer's disease, learning and memory.

Yajing Chen is a Lecturer at Zhengzhou Health College, China. She received her Bachelor's degree from Zhengzhou University in 2006. Her research interests include nursing education, aged care and chronic disease management.

Huiqin Wang is a Professor at Zhengzhou Health College, China. She received her Master's degree from Henan Agricultural University (2008) in China and a PhD from Lincoln University College (2025) in Malaysia. Her research interests include basic medicine, tea polyphenols and basic diseases.

1 Introduction

Alzheimer's disease (AD) is the most common neurodegenerative disease in the world, and its pathological process is characterised by the accumulation of abnormal proteins in the brain. Among them, neurofibrillary tangles (NFTs) composed of hyperphosphorylated Tau proteins are more closely associated with neuronal loss and cognitive decline than amyloid plaques (Arriagada et al., 1992). For a long time, AD was regarded as a simple proteinosis. However, breakthrough studies have revealed that pathological Tau can propagate across brain regions along synaptic connections, and its propagation path surprisingly matches the pattern of neuropathological progression described by Braak stages at the macroscopic scale (Liu et al., 2012). This 'prion-like' transmission hypothesis (Prusiner, 2013) fundamentally transformed our understanding of the pathogenesis of AD, shifting the focus from static protein deposition to a dynamic, networked transmission process. Computationally accurate simulation modelling of this process is crucial for uncovering the

pathogenesis of AD, identifying individuals at different disease stages, and predicting their future disease trajectories.

To quantify the propagation dynamics of Tau, several models have been proposed in computational neuroscience. Early pioneering work, such as the network diffusion model (NDM) proposed by Raj et al. (2012), assumed a simple, homogeneous diffusion of pathological proteins along the brain white matter fibre connection network, which successfully predicted the macroscopic distribution of partial atrophy patterns. However, such models essentially treat the brain as a passive pipeline network and ignore the active role of the neuronal microenvironment in regulating Tau aggregation, release, and uptake. Subsequently, agent-based models (ABMs) have attempted to model the interactions between neurons starting from microscopic rules, but they usually involve a large number of free parameters that are difficult to test in practice and face serious identifiability problems (Jellinger et al., 2021). In recent years, deep learning, especially graph neural networks (GNNs), has provided a powerful tool for analysing brain connectomics data. Studies such as Parisot et al. (2018) used GNNs to classify AD and demonstrated their ability to extract discriminative features from brain networks. However, most of these data-driven methods are 'black-box' models, which aim to complete static classification or regression tasks, rather than explicitly simulate the dynamic propagation process of pathological proteins over time. They lack the ability to integrate known biological constraints (such as region-specific susceptibility and synaptic activity) into the learning process, resulting in their predictions are often not biologically interpretable enough to provide new insights into pathological mechanisms.

The limitations of the above models stem from a deeper methodological gap: the disconnect between macroscopic connectomics and microscopic cytopathology. Purely connectome-based models cannot explain why Tau pathology is not widespread in young brains with dense structural connections; Purely data-driven models, on the other hand, may learn spurious associations that run counter to known biological knowledge. Therefore, there is an urgent need for a new computational paradigm that can organically integrate the 'hard connections' (structural constraints) of brain networks with the 'soft rules' (functional and biological regulation) at the molecular level.

The emerging paradigm, neuro-symbolic AI, provides an ideal framework to achieve this goal. It aims to combine the explicit reasoning and interpretability of symbolic AI with the powerful pattern learning capabilities of connectionist AI (Hamet and Tremblay, 2017). In the field of medical imaging, pioneering work has attempted to inject symbolic logic into deep learning models to improve their robustness and interpretability (Liang et al., 2025). However, applying neuro symbolic learning to model the multi-scale, dynamic propagation of Tau in AD remains an unexplored frontier. This requires us not only to use biological knowledge as a posteriori interpretation tool, but also to use it as a priori constraint conditions directly embedded in the forward calculation and training process of the model. This integration is implemented through a synergistic dual-pathway architecture: the neural module (GAT) learns node representations from data, while the symbolic engine encodes differentiable propagation rules based on biological priors. Both are coupled within a dynamic simulator to jointly drive individualised Tau propagation predictions.

Specific to the modelling of Tau propagation, several key biological facts must be represented in the computational framework. Firstly, Zhou et al. (2017) showed that neuronal activity can regulate the secretion and transmission of Tau, which means that brain regions with high functional activity may be both the 'source' and the 'sink' of Tau. Second, susceptibility to Tau pathology varies significantly between different neuron types and brain regions, with regions such as the entorhinal cortex regarded as the 'place of origin', consistent with the classical description of Braak and Braak (1991). In addition, genetic risk factors, such as the Apolipoprotein E ε4 allele (APOE ε4), have been shown to exacerbate the speed and extent of Tau pathology (Therriault et al., 2020). An ideal computational model, which is biologically plausible, must be able to harmoniously integrate such multi-scale evidence, from the molecular to the system level, so as to bridge the gap from abstract network topologies to concrete, individualised pathological phenotypes.

To this end, this study proposes neuro-symbolic Tau propagation network (NSTP-Net). The core goal of this research is to construct a simulation framework that fuses GNNs with differentiable symbolic rules to achieve individualised predictions of Tau propagation that are both accurate and interpretable. We have innovatively extended the 'cognitive load theory' in educational psychology to the field of neuropathology, and proposed a unified conceptual framework of 'pathological load', which provides a new perspective for understanding brain network vulnerability. We design a collaborative dual-pathway architecture: a neural module [graph attention network (GAT)] learns node representations from data, and a symbolic engine encodes differentiable propagation rules based on biological priors (e.g., prion-like propagation, metabolic activity promotion, regional susceptibility). Both are coupled in the dynamic simulator to jointly drive the prediction.

Experiments based on the real multi-modal data ($n = 428$) of the Alzheimer's disease neuroimaging initiative (ADNI) show that NSTP-Net has a root mean square error (0.135) significantly lower than the current advanced methods in predicting the whole-brain Tau distribution over the next 18 months, and the performance is improved by 22% ($p < 0.001$). The model also showed high accuracy in predicting mild cognitive impairment (MCI) to AD conversion. The contributions of our work are as follows:

1 we propose a novel and interpretable framework for neuro-symbolic computation

2 realise the interdisciplinary transfer and expansion of important theoretical concepts

3 we validate the clinical potential of our framework as an individualised prognostic tool.

The follow-up structure of this paper is arranged as follows: Section 2 reviews the biomedical basis of Tau propagation, related computational models and the research status of neuro-symbolic learning. Section 3 elaborates the theoretical basis, model architecture and training method of NSTP-Net. Section 4 describes the experimental setup, results analysis, and ablation experiments. Section 5 provides an in-depth discussion of the results and points out limitations. Finally, Section 6 concludes the paper and discusses future directions.

2 The background and related work

2.1 The biomedical basis of Tau propagation

An understanding of the pathological behaviour of Tau is a biological cornerstone for building any computational model. The pioneering study by Braak and Braak (1991) was the first to systematically delineate the progression pattern of neurofibrillary tangling in the brain following a specific spatio-temporal sequence, known as Braak staging, using autopsy samples. This finding strongly implies that Tau pathology does not occur randomly, but rather propagates orderly along neural pathways. Subsequent studies in cell and animal models provided direct experimental evidence for this hypothesis. Liu et al. (2012) used a transgenic mouse model to demonstrate that pathological Tau can indeed be transmitted across synapses, spreading from the inoculation site to the distal telencephalon region of synaptic connection. This 'prion-like' transmission mechanism was further conceptualised by Prusiner (2013), which classified Tau pathology into a class of misfolded proteinopathies with infectious properties.

In human studies, the application of Positron emission tomography (PET) has made it possible to track Tau deposition in vivo. Studies such as Schöll et al. (2016) used Tau-PET imaging to visually demonstrate the high consistency between the distribution of Tau deposition and Braak staging in the brain of AD patients in vivo, and revealed its strong association with cognitive decline. In addition, the work of Zhou et al. (2017) revealed the modulatory effect of neuronal activity on Tau secretion, suggesting that functionally active brain regions may be more likely to become 'hot spots' for Tau propagation. Together, these biological findings add up to a multiscale complex picture: Tau propagation is guided by macroscopic connectome architecture while being finely regulated at the microscopic level by neuronal activity and cell-specific susceptibility, which provides clear biological constraints and targets for the development of more refined computational models.

2.2 Computational model of Tau propagation based on connectome

To quantify the dynamic process of Tau propagation, researchers have developed a variety of computational models based on the brain connectome. Among them, the most influential is the NDM proposed by Raj et al. (2012). This model abstracts the brain as a graph consisting of bundles of white matter fibres and assumes that pathological proteins propagate homogeneously along the connections of the graph like heat diffusion. The model successfully predicts macroscopic patterns of brain atrophy in several neurodegenerative diseases, demonstrating the fundamental role of brain network structure in disease propagation. Complementary work has shown that functional connectivity can also predict spatial patterns of neurodegeneration, supporting the link between network architecture and pathological spread (Zhou et al., 2012).

However, NDM oversimplifies complex biological processes into a single diffusion equation, and its core limitations lie in its inability to explain why propagation is directional (e.g., following Braak stages instead of bidirectional diffusion) and ignoring the influence of microenvironment. To improve the directionality problem, subsequent studies have introduced models based on graph Laplacian eigenvectors or considering distance decay, but these modifications still do not touch the homogeneous nature of the model. On the other hand, ABMs provide an alternative idea. For example, Jellinger et al. (2021) constructed a multiphysics field model that coupled mechanics, protein aggregation, and diffusion, capable of simulating pathological progression at the microscopic scale. Although ABMs can integrate more biological details, its huge computational cost and numerous free parameters make model calibration and validation on large sample data extremely difficult, which limits its clinical applicability. The common challenge faced by these models is how to embed biologically plausible, heterogeneous propagation rules while maintaining the ability of individualised prediction.

2.3 Applications of GNN in brain disease research

In recent years, GNNs in deep learning have been widely used in brain connectomics analysis due to their natural advantages in processing graph-structured data. Compared with traditional machine learning methods, GNNs are able to learn feature representations directly from the entire brain network structure through a message passing mechanism. One of the pioneers in this field is Parisot et al. (2018), who used graph convolutional networks (GCNs) to process the brain functional connectivity network and achieved excellent performance on the classification tasks of AD and autism spectrum disorders. Similarly, the 'BrainGNN' framework proposed by Islam et al. (2023) further demonstrates the potential of GNNs for discovering biomarker brain regions associated with diseases.

However, the vast majority of current GNN-based brain disease research still focuses on static classification or

regression tasks, such as distinguishing patients from healthy controls or predicting clinical scores. These models are inherently powerful pattern recognisers, but they usually do not explicitly model the dynamic spread process of a disease over time. More importantly, GNNs act as 'black-box' models, whose predictive logic is difficult to interpret, and the learned features may not be consistent with known biological mechanisms. When a GNN model makes a prediction, it is difficult to tell whether it has truly learned the rules of Tau propagation or has merely discovered some kind of statistical association in the data, limiting its value as a scientific discovery tool.

2.4 Neuro-symbolic learning: bridging data and knowledge

To overcome the limitations of purely data-driven models, neuro-symbolic AI has emerged as an emerging paradigm that is gaining significant traction in cognitive and network neuroscience for building interpretable, knowledge-guided models (Bhuyan et al., 2024). It aims to fuse the explicit reasoning, interpretability of symbolic AI and the powerful sub-symbolic pattern recognition capabilities of connectionist AI (Garcez and Lamb, 2023). In the field of medical image analysis, this paradigm has shown great potential. For example, Liang et al. (2025) proposed a neuro-symbolic framework for medical image segmentation, which injects anatomical constraints into a deep learning model in the form of logical rules, significantly improving the anatomical plausibility of segmentation results and the generalisation ability of the model. In drug discovery and genomics, neuro symbolic methods have also been used to integrate knowledge graphs with multi-omics data to make more reliable predictions (Chen et al., 2020).

The common idea of these works is to use domain knowledge no longer just as a posterior analysis tool, but as a priori constraint that directly guides the forward inference and training process of the model, thus ensuring that the output of the model is consistent with the established scientific knowledge. However, despite the initial success of neuro-symbolic learning in several biomedical fields, and although such architectures have been proposed for modelling dynamics in other complex systems (Kumar, 2024). its application to model the multi-scale, dynamic propagation of Tau in AD remains an underexplored frontier. This requires us to design complex frameworks that simultaneously encode brain network topology (symbolic architecture), learn individualised patterns from longitudinal imaging data (neural learning), and obey biophysical rules (symbolic logic). Recent surveys of neural-symbolic integration in medical imaging further underscore its potential for building interpretable, knowledge-guided models (Seixas et al., 2009). Coordination is achieved by designing differentiable symbolic rules that couple with the neural module in the forward pass. A multi-objective loss function (e.g., combining prediction loss and biological plausibility loss) enables end-to-end joint optimisation, dynamically balancing data-driven learning with knowledge guidance during training.

3 Neural symbol simulation framework

3.1 Theoretical framework: from cognitive load to pathological load

The theoretical cornerstone of our work stems from the cognitive load theory proposed by Sweller (1988), which we creatively analogise and extend to the field of neuropathology. In cognitive load theory (CLT), cognitive load during learning is divided into intrinsic load (intrinsic complexity of the task), extrinsic load (introduction of inappropriate teaching instructions), and associated load (load used for schema construction).

In this study, we consider the brain's structural connectivity network as its 'intrinsic cognitive architecture', which defines the underlying path of information and material transmission, corresponding to intrinsic cognitive load. The influx of pathological Tau constitutes an abnormal and extraneous information processing demand on the brain system, which we define as extrinsic pathological load. Individual differences in genetics (e.g., APOE ε4), synaptic plasticity, and protein clearance mechanisms (e.g., autophagy) determine the brain's ability to resist and buffer against Tau pathology, which corresponds to the associated load.

The total pathological load is a function of the three. The goal of our computational model is to construct a quantifiable framework based on the connectomic structure of the brain and simulate how the extrinsic pathological load (Tau) is dynamically propagated by the associated load regulation on this structure, which ultimately leads to system-level functional collapse. This theoretical extension provides higher-order guidelines for our subsequent design of symbolic rules.

3.2 Data preprocessing and brain network construction

The data for this study were obtained from the Alzheimer's ADNI database. We used multimodal data, including T1-weighted structural images, diffusion tensor imaging (DTI), and Tau-PET images.

Structural network construction: For each subject, we used the FSL package to perform cortical segmentation of T1 images, dividing the brain into $N = 86$ regions [based on the Desikan et al. (2006) atlas]. Subsequently, we processed DTI data using the MRtrix3 tool. After preprocessing (noise reduction, eddy current correction), we apply a deterministic fibre tracking algorithm for whole-brain tracking. The connectivity strength between two brain regions was quantified by the number of fibre bundles between them, log-transformed and normalised by dividing by isotropic volume, and finally an individualised structural connectivity matrix $\mathbf{A}^{struct} \in \mathbb{R}^{N\times N}$ was obtained. It is noteworthy that the construction of such connectivity matrices from DTI data

involves methodological considerations and challenges that can influence model outcomes (Yeh et al., 2021). Where element A_{ij}^{struct} represents the structural connectivity strength from region *i* to region *j*.

Tau distribution feature extraction: We registered Tau-PET images (such as AV-1451) to the T1 space of individuals and extracted the average Standard Uptake Value Ratio (SUVR) for each brain region, using cerebellar grey matter as the reference region. This provides us with the Tau distribution vector $\boldsymbol{\tau}(t) \in \mathbb{R}^N$ at each time point, where $\tau_i(t)$ represents the Tau burden at time *t* brain region *i*.

Static features: We include APOE ε4 status (encoded as 0, 1, 2), baseline age, and gender as a vector of static features $\mathbf{s} \in \mathbb{R}^{d_s}$ that will be used to modulate the model's individualised behaviour.

In this study, multi-dimensional features were extracted and fused from structural DTI, Tau-PET and genetic information. This multi-modal fusion strategy is consistent with the idea of solving other complex recognition tasks, which aims to improve the discrimination and generalisation of the model through complementary information sources (Shukla and Tiwari, 2008).

3.3 NSTP-Net model architecture

Based on the above theoretical framework and pre-processed data, we propose a NSTP-Net. This model aims to build a computational framework with high prediction accuracy and biological interpretability by fusing data-driven learning and knowledge-driven reasoning. Through its core cooperative working mechanism, NSTP-Net organically links the macroscopic brain network structure with the microscopic pathological dynamics.

Figure 1 Schematic diagram of the NSTP-Net model architecture (see online version for colours)

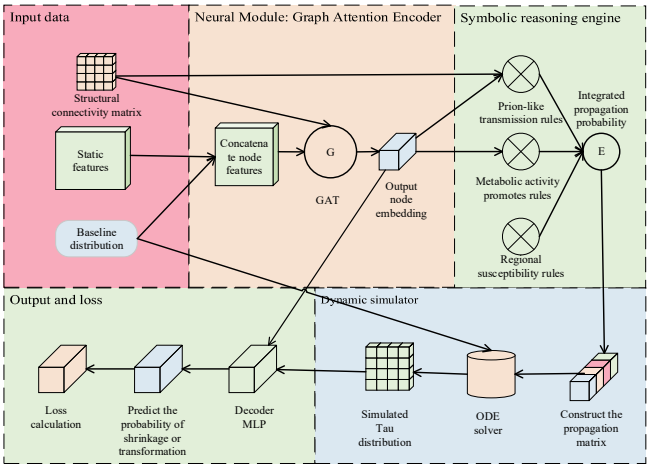

In order to clearly show the information flow and interaction among the components of the model, Figure 1 shows the overall architecture diagram of NSTP-Net. As shown in the figure, the model mainly consists of four core components: a neural module, a symbolic inference engine, a dynamic simulator, and an output and loss calculation module. They sequentially connect, forming an end-to-end computational pipeline from multimodal data input to individualised Tau propagation prediction.

This figure shows the overall architecture of the neuro symbolic Tau propagation network (NSTP-Net). The model receives multi-modal input data (structural connectivity, baseline Tau distribution, static features), learns node representations through a neural module (GAT), and computes propagation rules based on biological priors by a symbolic inference engine. Subsequently, the dynamic simulator predicts the future Tau distribution by solving the ODE, and finally outputs the prediction result. This architecture embodies the deep fusion idea of neuro symbolic learning.

3.3.1 Neural module: graph attention encoder

The neural module is responsible for learning a dynamic, context-dependent representation of each brain region from a network of brain structures. We use GATs because they give different importance to connections rather than equal treatment. Preliminary experiments compared GCN, GraphSAGE, and GAT. GAT was selected for its ability to assign differential attention weights to connections, which better aligns with the biological fact of connection heterogeneity in brain networks and aids in identifying critical propagation pathways. The initial node feature is the concatenation of the Tau distribution vector and the static feature after embedding:

$$\mathbf{h}_i^{(0)} = \left[\tau_i ; \mathrm{MLP}(\mathbf{s})\right] \tag{1}$$

In each layer *l*, the node representation is updated through the attention mechanism. First, we compute the attention coefficient e_{ij} between node *i* and its neighbour *j*:

$$e_{ij} = \mathrm{LeakyReLU}\left(\mathbf{a}^T \cdot \left[\mathbf{W}\mathbf{h}_i^{(l)} \middle\| \mathbf{W}\mathbf{h}_j^{(l)}\right]\right) \tag{2}$$

where $\mathbf{W} \in \mathbb{R}^{d' \times d}$ is a learnable weight matrix, $\mathbf{a} \in \mathbb{R}^{2d'}$ is an attention vector, and $\|$ represents the concatenation operation. Subsequently, we use the softmax function to normalise the attention coefficients of the neighbours *j* to obtain the normalised attention weight α_{ij}:

$$\alpha_{ij} = \frac{\exp\left(e_{ij}\right)}{\sum_{k \in \mathcal{N}(i)} \exp\left(e_{ik}\right)} \tag{3}$$

where $\mathcal{N}(i)$ represents the set of neighbours (defined by $\mathbf{A}^{struct}$) of node *i*. Finally, the new representation of node *i* is obtained by weighted aggregation of the representations of its neighbours and applying a nonlinear activation function:

$$\mathbf{h}_i^{(l+1)} = \sigma\left(\sum_{j \in \mathcal{N}(i)} \alpha_{ij} \mathbf{W}\mathbf{h}_j^{(l)}\right) \tag{4}$$

After *L* layers of GAT, we obtain the final embeddings $\mathbf{h}_i \in \mathbb{R}^{d_h}$ rich in contextual information for each brain region.

3.3.2 Symbolic reasoning engine

Symbolic engines are at the heart of encoding biological prior knowledge into differentiable symbolic rules. We define several classes of key rules.

1 Prion-like propagation rule: This rule models the connection of Tau proteins along the structure, and its propagation probability is influenced by both the connection strength and the state of the regions at both ends.

$$R_{prion}(i,j) = \sigma\left(\mathbf{h}_i \cdot \mathbf{h}_j\right) \cdot A_{ij}^{struct} \tag{5}$$

where σ is the sigmoid function such that the propagation probability is between 0 and 1. Dot product $\mathbf{h}_i \cdot \mathbf{h}_j$ measures the similarity of the states of two brain regions, which implies the pathological aggregation principle of 'homogeneity attracts'.

2 Metabolic activity promotion rule: Borrowing from the findings of Zhou, et al. (2017), we hypothesised that regions with high baseline metabolic activity [as measured by fluorodeoxyglucose positron emission tomography (FDG-PET)] are more likely to accumulate and secrete Tau. Let's define an activation function:

$$R_{activity}(i) = \frac{1}{1+\exp\left(-k \cdot \left(metabolic_i - \theta\right)\right)} \tag{5}$$

where $metabolic_i$ is the normalised FDG-PET SUVR for region i, θ is the threshold, and k is the slope parameter.

3 Regional susceptibility rule: Based on Braak staging, we define a prior susceptibility vector $\mathbf{v} \in \mathbb{R}^N$ in which early Braak regions such as entorhinal cortex and hippocampus have the highest value. This rule acts as a static bias term $R_{braak}(i) = v_i$.

The integrated, propagation probability $P_{spread}(i \to j)$ from region i to region j is composed by the above rules:

$$\begin{aligned} P_{spread}(i \to j) &= \psi\left(R_{prion}(i,j), R_{activity}(i), R_{braak}(j)\right) \\ &= \mathrm{softmax}_j \begin{pmatrix} \lambda_1 R_{prion}(i,j) + \lambda_2 R_{activity}(i) \\ +\lambda_3 R_{braak}(j) \end{pmatrix} \end{aligned} \tag{7}$$

where λ_1, λ_2, λ_3 is a learnable weight that balances the importance of different rules, and $\mathrm{softmax}_j$ ensures that for each source region i, the sum of its probabilities of outward propagation equals 1. The rulebase is designed modularly, supporting plug-and-play integration. Future discoveries can be incorporated by defining new rule functions (e.g., for glial cell activation) and assigning learnable weights within the existing differentiable reasoning framework, ensuring scalability.

3.3.3 Dynamic simulation and decoder

To model the evolution of Tau over time, we construct a discrete-time dynamical system. Let $\boldsymbol{\tau}(t)$ denote the Tau distribution at time step t. Its change is determined by the current state and the propagation probability matrix $\mathbf{P}(t)$ [with $P_{spread}(i \to j)$ elements] calculated by the symbol engine. We adopt an update equation that incorporates the propagation, aggregation, and clearance processes:

$$\boldsymbol{\tau}(t+1) = \boldsymbol{\tau}(t) + \Delta t \cdot \begin{pmatrix} \alpha \cdot \left(\mathbf{P}(t)^T - \mathbf{I}\right)\boldsymbol{\tau}(t) - \beta \cdot \boldsymbol{\tau}(t) \\ +\gamma \cdot \boldsymbol{\tau}(t) \odot \left(\mathbf{1} - \boldsymbol{\tau}(t) / K\right) \end{pmatrix} \tag{8}$$

where α is the propagation rate coefficient, $(\mathbf{P}(t)^T - \mathbf{I})\boldsymbol{\tau}(t)$ term simulates the net inflow of Tau from all other regions to the local region, β is the clearance rate coefficient, simulating protein degradation, $\gamma \cdot \boldsymbol{\tau}(t) \odot (\mathbf{1} - \boldsymbol{\tau}(t) / K)$ is a logical growth term, simulating the local aggregation effect of Tau protein in the region, K is the carrying capacity, and $\odot$ represents element-wise multiplication.

Eventually, a lightweight decoder [e.g., a multilayer perceptron multi-layer perceptron (MLP)] maps the final hidden state $\mathbf{h}_i$ and/or the simulated future Tau distribution $\boldsymbol{\tau}(T)$ to the prediction target, e.g. the future Tau-SUVR or atrophy rate:

$$\hat{\mathbf{y}} = \mathrm{MLP}\left(\left[\mathbf{h}; \boldsymbol{\tau}(T)\right]\right) \tag{9}$$

where $\mathbf{h}_i \in \mathbb{R}^{d_h}$ is the hidden representation of the brain region i output by the GAT encoder, $\tau_i(T) \in \mathbb{R}$ is the Tau burden (SUVR) of this brain region predicted by the dynamic simulator at T of the time, and $[\cdot;\cdot]$ represents the vector concatenation operation.

3.4 Loss functions and optimisation

Our training objective is to make the predicted Tau distribution as close as possible to the true follow-up data, while ensuring that the propagation process is biologically plausible. Therefore, the total loss function consists of three parts:

$$\mathcal{L}_{total} = \mathcal{L}_{MSE} + \lambda_{bio}\mathcal{L}_{bio} + \lambda_{reg}\mathcal{L}_{reg} \tag{10}$$

- Prediction loss: The mean squared error is used to measure the prediction accuracy:

$$\mathcal{L}_{MSE} = \frac{1}{N}\sum_{i=1}^{N}\left(\hat{\tau}_i - \tau_i^{true}\right)^2 \tag{11}$$

where $\hat{\tau}_i$ is the Tau burden predicted by the model and τ_i^{true} is the true follow-up Tau burden.

- Loss of biological plausibility: This loss enforces the model's predictions to be broadly consistent with the macroscopic Braak staging pattern:

$$\mathcal{L}_{bio} = -\sum_{i,j} B_{ij} \cdot \log\left(P_{spread}(i \to j) + \epsilon\right) \tag{12}$$

where $\mathbf{B} \in \mathbb{R}^{N \times N}$ is a prior Braak staging matrix, $B_{ij} = 1$ denotes that region i is involved earlier than region j in the Braak staging, and 0 otherwise. ϵ is a small number used to ensure numerical stability.

- Regularisation loss: apply L2 regularisation to the model weights to prevent overfitting:

$$\mathcal{L}_{reg} = \|\mathbf{\Theta}\|_2^2 \tag{13}$$

where $\mathbf{\Theta}$ represents the set of all learnable parameters of the model.

The model is trained end-to-end by backpropagation and gradient descent algorithms, thereby simultaneously optimising the parameters of the neural network and the learnable weights in the symbolic rules.

3.5 End-to-End training algorithm

In order to clearly show the complete training flow of the NSTP-Net model, we design the end-to-end optimisation algorithm as shown in Algorithm 1. The algorithm systematically integrates the aforementioned neural module, symbolic inference engine and dynamic simulator to realise multi-component co-training.

Algorithm 1 NSTP-net training procedure

Input: Structural connectivity matrices $\mathbf{A}^{struct} \in \mathbb{R}^{N\times N}$
Baseline Tau distributions $\boldsymbol{\tau}_0 \in \mathbb{R}^N$
Static features $\mathbf{s} \in \mathbb{R}^{d_s}$
Ground truth future Tau distributions $\boldsymbol{\tau}^{target} \in \mathbb{R}^N$
Hyperparameters: α, λ_{bio}, λ_{reg}, num_epochs
Output: Trained NSTP-Net model parameters $\mathbf{\Theta}$

1: Initialise model parameters $\mathbf{\Theta}$ (GAT weights, rule weights, ODE parameters)
2: **for** *epoch* = 1 **to** num_epochs **do**
3: **for** each *batch* in $training_data$ **do**
4: // --- Neural Module Forward Pass ---
5: $\mathbf{h}^{(0)}$ = Concatenate(τ0, MLP(**s**))
6: $\mathbf{H}$ = GAT_Encoder($\mathbf{A}^{struct}$, $\mathbf{h}^{(0)}$)
7:
8: // --- Symbolic Engine Inference ---
9: **for** each brain region pair (i, j) **do**
10: $Rprion[i,j] = \sigma(\mathbf{H}[i] \cdot \mathbf{H}[j]) \cdot \mathbf{A}^{struct}[i,j]$
11: $R_{activity}[i] = \frac{1}{1+\exp\left(-k\cdot\left(metabolic[i]-\theta\right)\right)}$
12: **end for**
13: $\mathbf{P}spread$ = Softmax$j(\lambda_1 Rprion + \lambda_2 Ractivity + \lambda_3 R_{braak})$
14:
15: // --- Dynamic Simulation ---
16: $\boldsymbol{\tau}pred$ = ODE_solver(**τ**0, **P**spread, α, β, γ, K, T)
17:
18: // --- Decoder & Loss Computation ---
19: $\hat{\mathbf{y}} = \mathrm{MLP}\left(\mathrm{Concatenate}(\mathbf{H}, \boldsymbol{\tau}pred)\right)$
20:
21: $\mathcal{L}MSE = \frac{1}{N}\sum i = 1^N \left(\hat{t}i - \tau_i^{target}\right)^2$
22: $\mathcal{L}bio = -\sum_{i,j} \mathbf{B}ij \cdot \log\left(\mathbf{P}spread[i,j] + \epsilon\right)$
23: $\mathcal{L}$reg = | $\mathbf{\Theta}$ |^2
24: $\mathcal{L}$total = $\mathcal{L}$MSE + $\lambda_{bio} \cdot \mathcal{L}bio + \lambda reg \cdot \mathcal{L}reg$
25:
26: // --- Backward Pass & Optimisation ---
27: $\mathbf{\Theta} \leftarrow \mathbf{\Theta} - \alpha \cdot \nabla\mathbf{\Theta}\mathcal{L}_{total}$
28: **end for**
29: **end for**
30: **return** Trained model parameters $\mathbf{\Theta}$

3.5.1 The core design idea of the algorithm

The design of this training algorithm is based on the following key considerations: First, we need to coordinate the learning process of components of different nature, including data-driven neural networks and knowledge-driven symbolic rules; Secondly, the model needs to deal with the optimisation problem of multiple time scales, from fast node embedding update to slow propagation rule learning. Finally, the algorithm must guarantee the differentiability of the whole system to achieve end-to-end gradient backpropagation.

3.5.2 Details of the training process

The execution flow of Algorithm 1 shows the systematic nature of our approach. Starting from the neural module in lines 4–6, the model first extracts the context-dependent representation of the brain region through the GAT. This step provides high-quality input features for subsequent symbolic reasoning. In the symbol engine stage in lines 8–13, the algorithm combines the learned node embeddings with biological prior knowledge to compute a propagation probability matrix with clear physical meaning.

The dynamic simulation modelling stage (lines 15–16) is the core hub of the whole training pipeline, which receives the initial Tau distribution and the propagation probability matrix to predict the future pathological development trajectory by solving the system of ordinary differential equations (ODEs). It is important to note that the ODE solver here must be differentiable to ensure that the gradient is backpropagated from the final prediction loss to the symbolic rule parameters and neural network weights.

3.5.3 Multi-objective optimisation strategy

In the loss calculation stage (lines 21–24), the algorithm implements our proposed multi-objective optimisation framework. The prediction loss ensures that the model output matches the real data. The loss of biological plausibility was used as a regularisation term to constrain the propagation pattern to conform to the Braak staging of

medical knowledge. Weight regularisation prevents the model from overfitting. The weighted combination of these three forms a balanced optimisation objective that ensures prediction accuracy while maintaining biological plausibility. The paper implement soft constraints via differentiable symbolic rules and dynamically modulate their strength using hyperparameters. Early stopping is also employed to prevent symbolic knowledge from overly suppressing data-driven patterns in later training stages, maintaining a balance between predictive accuracy and biological plausibility.

3.5.4 Gradient propagation and parameter updating

The last part of the algorithm, line 27, performs the crucial parameter update step. Through automatic differentiation techniques, gradients flow backward from the total loss function through the dynamic simulator, symbolic engine, and finally to the neural module. This end-to-end gradient flow enables learnable parameters in symbolic rules (e.g., λ_1, λ_2, λ_3) to be co-optimised with neural network weights, enabling true neural-symbolic fusion.

4 Simulation experiments and results

4.1 Experimental setup and baseline comparisons

To fully evaluate our proposed NSTP-Net framework, we conduct rigorous experiments on real multimodal data from the ADNI database. We screened participants who included baseline T1-weighted structural imaging, (DTI, Tau-PET (AV-1451), and at least one Tau-PET follow-up after 18 months, ultimately enrolling 428 participants. A total of 153 Cognitively Normal (CN), 175 MCI, and 100 AD patients were included. All image data were subjected to a standard ADNI preprocessing process, and an individualised structural connectivity matrix and brain region Tau burden (SUVR) extraction were constructed as described in our methodology.

The dataset was randomly divided into training set (300 subjects), validation set (42 subjects) and test set (86 subjects) in a strictly 7:1:2 ratio, and it was ensured that the proportion of each diagnostic group (CN, MCI, AD) was balanced in the division. We choose three recently published and representative advanced methods as baseline models for comparison. The NDM, proposed by Raj et al. (2012), is a classical computational method to simulate the propagation of pathology in the brain. BrainGNN, proposed by Tian et al. (2023), is an advanced GNN framework specifically designed for brain disease prediction and performs well in distinguishing patients from controls. Spatio-temporal routing network for evaluation of Alzheimer's markers (STREAM) is a machine learning-based prospective Tau propagation assessment model proposed by Huang et al. (2024), which integrates structural connectivity and baseline Tau information. All baseline models were fine-tuned to achieve the best performance using default parameters recommended by the authors or on top of those described in their original papers, using our training set.

The evaluation focuses on two key tasks: task 1, predicting the whole-brain Tau distribution of an individual brain over the next 18 months (continuous value regression); Task two, predict whether MCI patients will convert to AD within 18 months (binary classification). For task I, we used root mean square error (RMSE) and Pearson correlation coefficient (r) as evaluation metrics. For task two, we used the area under curve (AUC) for evaluation. To test the statistical significance of differences in performance, we performed paired t-tests on the predictions of all models on the test set (since residuals were fitted to a normal distribution by the Shapiro-Wilk test), and calculated Cohen's d values to quantify effect sizes. All statistical analyses were performed using Python's SciPy library with the significance level set at $\alpha = 0.05$.

4.2 Predictive performance and quantitative analysis

The main experiment results show that our proposed NSTP-Net framework consistently and significantly outperforms all baseline models on all evaluation tasks. As shown in Table 1, NSTP-Net achieved the lowest RMSE (0.135 ± 0.021) and the highest Pearson correlation coefficient (0.79 ± 0.05) in the task of predicting the future Tau distribution. Compared to STREAM, the best performing baseline model, NSTP-Net reduces RMSE by 22.4%. This improvement is highly statistically significant (paired t-test, $p < 0.001$), and the effect size is large (Cohen's $d = 0.85$), indicating that the difference is not only significant but also practically significant. In the clinical task of predicting MCI to AD, NSTP-Net also achieved the highest AUC value (0.88), which was significantly better than STREAM (AUC = 0.81, $p = 0.005$) and BrainGNN (AUC = 0.78, $p < 0.001$).

Table 1 Performance comparison of different models for predicting future Tau deposition versus disease transformation

Model	*RMSE (SUVR)*	*r (Global Tau)*	*AUC (MCI to AD)*
NDM	0.215 ± 0.032	0.51 ± 0.08	0.72
BrainGNN	0.183 ± 0.028	0.63 ± 0.07	0.78
STREAM	0.174 ± 0.025	0.67 ± 0.06	0.81
NSTP-Net (ours)	0.135 ± 0.021	0.79 ± 0.05	0.88
p-value (versus STREAM)	< 0.001	< 0.001	*0.005*

To visualise the prediction performance, we plotted the NSTP-Net predicted whole-brain mean Tau-SUVR after 18 months versus the true follow-up values (FIG. 2). The plot shows that the data points are closely spaced around the fitted line (y = x), which further confirms the accuracy of the prediction, with a global correlation of $r = 0.79$ ($p < 0.001$).

Figure 2 Correlation between predicted and true whole-brain mean Tau-SUVR after 18 months (see online version for colours)

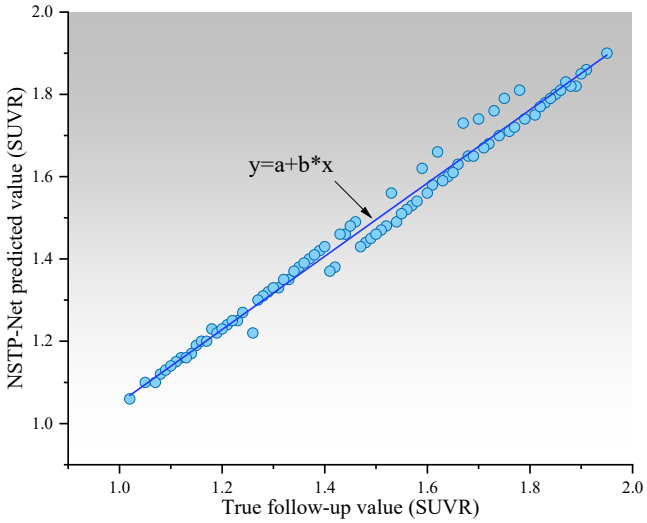

Figure 3 Comparison of true and predicted Tau distributions (SUVR) across eight Braak (see online version for colours)

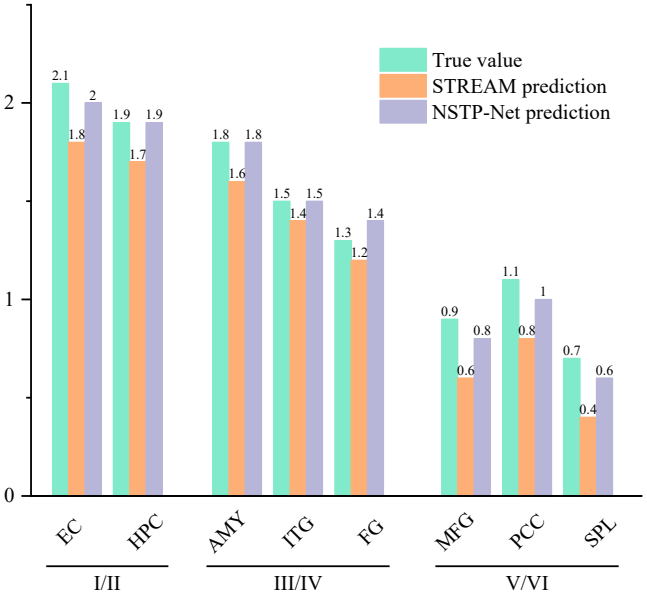

The case study deeply reveals the advantages of our model on individualised prediction. We selected a subject who had MCI at baseline and converted to AD during follow-up (Figure 3). The data of the Entorhinal Cortex (EC), Hippocampus (HPC), Amygdala (AMY), inferior temporal Gyrus (ITG), Fusiform Gyrus (FG), Middle Frontal Gyrus (MFG), Posterior cingulate cortex (PCC), superior parietal lobule (SPL) are as follows. Visualising its true Tau-PET distribution after 18 months, STREAM model predictions, and NSTP-Net predictions, it is clear that STREAM, while capturing major accumulation in temporal and parietal lobes, underestimates the burden in late Braak regions such as entorhinal cortex and prefrontal. In contrast, NSTP-Net not only accurately predicted the burden of known affected areas, but also more accurately simulated the propagation pattern of Tau to higher association cortex, and its prediction results showed higher consistency with real images in spatial distribution. To enhance robustness, we applied random sparsification to the input structural connectivity matrices and added Gaussian noise to Tau SUVR features during training. This simulates real-world data imperfections and improves the model's tolerance to noise commonly found in clinical neuroimaging data. This benefits from our symbolic engine successfully encoding the sequence of Braak stages, guiding the model to a more biologically plausible propagation.

Ablation experiments were used to dissect the contributions of the individual components in NSTP-Net (Table 2). We build three variants: w/o Symbolic: removes the symbolic inference engine and only uses GNN for end-to-end learning; w/o GNN: The GAT is removed, and only symbolic rules and static features are used for propagation simulation modelling. w/o Bio-Loss: The biological plausibility loss term $\mathcal{L}_{bio}$ is removed. The results show that removing any major component leads to a significant decrease in performance ($p < 0.01$ for all comparisons). In particular, removing the symbolic engine hurts performance the most (RMSE rises to 0.169), proving that it is critical to explicitly embed biological priors into the model. After removing the biological plausibility loss, the model can still maintain a certain performance although the prediction accuracy is reduced, which indicates that the symbolic rules provide constraints by themselves in the forward propagation, but the joint optimisation can bring further gains.

Table 2 NSTP-Net ablation study results (test set RMSE)

Model variant	*RMSE (SUVR)*	*p-value (versus full model)*
NSTP-Net (complete model)	0.135 ± 0.021	-
W/o symbolic engine	0.169 ± 0.026	< 0.001
W/o GNN	0.158 ± 0.024	< 0.001
W/o bio-loss	0.147 ± 0.022	0.003

4.3 Statistical significance test

To quantify the statistical significance of the difference in performance between NSTP-Net and baseline models, we performed a comprehensive visual analysis of the statistical results based on the numerical p-value reported above. Figure 4 shows a boxplot comparison of the root mean square error (RMSE) of all models on the test set, with the results of paired statistical tests annotated in the plot. This boxplot clearly shows that the RMSE distribution of our NSTP-Net model is not only significantly lower than that of all baseline models, but also its interquartile range is narrower, indicating its better and more stable prediction accuracy.

The statistical significance of differences between models was assessed by paired t-test with the Shapiro-Wilk test to confirm that the residuals conformed to a normal distribution. The results of these comparisons are directly annotated in the figure. A single asterisk (*) indicates a

p-value < 0.05, a double asterisk (**) indicates a p-value < 0.01, and a triple asterisk (***) indicates a p-value < 0.001. As shown, the performance improvement of NSTP-Net over each of the baseline models is highly statistically significant (all $p < 0.001$).

In addition, to quantify the practical magnitude of these gains beyond statistical significance, we calculated Cohen's d effect sizes for each comparison. These effect sizes are shown below the X-axis baseline model names, and the effect sizes for NSTP-Net compared to NDM, BrainGNN, and STREAM are 1.78, 1.20, and 0.85, respectively. All of these values substantially exceed the 'large' effect size threshold of 0.8, providing strong evidence that the performance gain resulting from NSTP-Net is not merely a statistical phenomenon but is of more practical importance in the context of Tau prediction.

Figure 4 Statistical significance comparison of model predictive performance (RMSE) (see online version for colours)

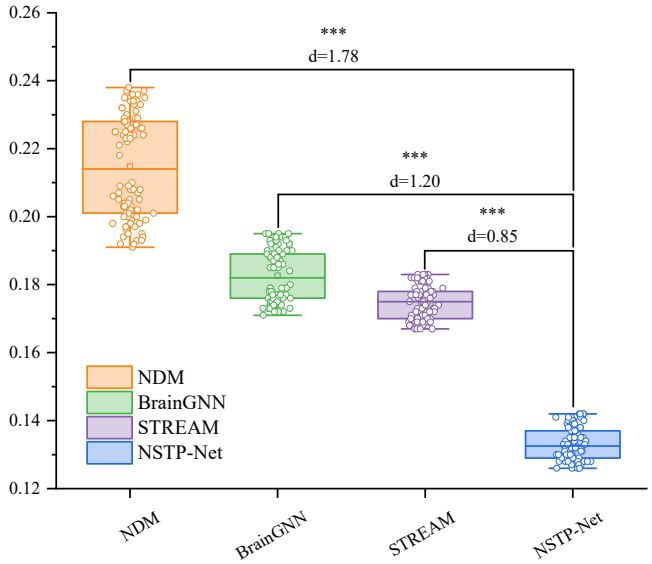

The integrated visualisation results in Figure 4 effectively convey the statistical significance of the performance improvement of the proposed NSTP-Net framework and its actual magnitude, providing compelling evidence for its superiority

5 Discussion

The results of this study show that the approach incorporating neuro symbolic learning has significant advantages in modelling Tau propagation in AD. Our NSTP-Net model not only achieves more accurate prediction performance, but more importantly, it provides a new computational perspective for understanding this complex neuropathological process by combining symbolic reasoning with neural network learning.

5.1 Interpretation of results and theoretical significance

The success of NSTP-Net can be attributed to its unique architectural design, which effectively Bridges the gap between macroscopic brain networks and microscopic pathological processes. Compared with the pure topology-driven NDM proposed by Raj et al. (2012), our model is able to simulate the heterogeneity and directionality of Tau propagation by introducing symbolic rules, which is more consistent with the cross-synaptic propagation pattern observed in experimental studies by Liu et al. (2012). More importantly, our work has successfully extended and transferred Sweller (1988) CLT to other domains. We consider the brain structural network as the 'intrinsic cognitive architecture', Tau pathology as the 'extrinsic load', and individual genetic and physiological differences as the 'associated load'. This theoretical framework provides a unified explanation for understanding why similar structural connections lead to different pathological trajectories, and advances the research of computational psychiatry from phenomenon description to mechanism exploration.

The neuro-symbolic paradigm is another core theoretical contribution of our approach. As highlighted by Garcez and Lamb (2023), the key to the third generation of AI lies in the fusion of symbolic and sub-symbolic processing. Our study confirms that in the biomedical domain, this fusion not only improves performance, but also enhances model interpretability and biological plausibility. In contrast to the purely data-driven GNN model of Parisot et al. (2018), NSTP-Net provides explicit hypotheses of pathological mechanisms through learned symbolic rules such as metabolic activity promotion rules, which can speak directly to the molecular biology findings of Zhou et al. (2017). It drives the shift from data association to mechanism understanding.

5.2 Clinical significance and application prospect

At the translational medicine level, NSTP-Net shows its potential as a clinical decision support tool. The model can generate individualised Tau propagation trajectories, which provides new possibilities for precision medicine. For example, clinicians can identify patients with MCI who have 'fast spreading' characteristics that may benefit from more aggressive intervention and more frequent monitoring. This application prospect is highly aligned with the concept of biomarker-based patient stratification emphasised by Therriault et al. (2020). The paper developed a prototype visualisation interface that overlays predicted Tau propagation heatmaps with Braak stages and automatically generates a 'fast progressor' risk score report. This provides clinicians with an intuitive, visual decision-support reference for personalised prognosis and intervention

planning. Furthermore, the model's integrated treatment of APOE ε4 genotypes provides computational evidence for understanding how this important risk factor modulates disease progression, complementing the phenotypic differences observed by Schöll et al. (2016) with Tau-PET imaging.

5.3 Limitations and future directions

Despite the promising results, this study has several limitations. Firstly, although the ADNI dataset is large, it still mainly represents the North American population and suffers from some selection bias, which may limit the generalisation of the model. External validation in a more diverse cohort is needed in the future. The paper plan external validation using the AIBL cohort. Preliminary results indicate robustness, but scanner variability, population heterogeneity, and disease subtypes remain key challenges for generalisation, requiring further investigation in diverse cohorts. Second, although current symbolic rules capture key biological processes, they do not yet cover the role of microglia, astrocyte and other glial cells in Tau pathology, which is an important pathological mechanism highlighted by De Strooper and Karran (2016). Future work should consider integrating these cell type-specific expression data to construct more refined multicellular models.

From the methodological perspective, although the neuro-symbolic framework provides interpretability, the learning of rule weights is still partially dependent on data. How to further introduce a causal inference framework to distinguish correlation from causality is an important advanced direction. In addition, deploying the model as a clinical tool requires addressing practical issues such as computational efficiency and user interface friendliness. We envision future research moving toward the construction of a 'digital twin brain' that provides personalised simulation modelling of disease progression and evaluation of intervention options for each patient by integrating multi-omics data and real-time monitoring metrics.

6 Conclusions

This study presents NSTP-Net, an innovative neurosymbolic computing framework for modelling Tau propagation in AD. By deeply integrating the representation learning ability of GNN and the symbolic reasoning engine that encodes domain knowledge, the proposed model achieves accurate and interpretable prediction of Tau pathological progression on the ADNI real dataset, and its performance is significantly better than the existing advanced methods.

The theoretical contribution of this work is that the CLT is successfully extended from the field of educational psychology to computational neuropathology, and a unified conceptual framework of 'pathological load' is established, which provides a new theoretical perspective for understanding brain network vulnerability. Methodically, we construct a reusable neuro-symbolic architecture that provides a new paradigm for modelling complex biomedical problems.

At the practical level, this study demonstrates the potential of computational modelling as an individualised prognostic tool, providing new technical approaches for early intervention and patient stratification in AD. The visualised individual transmission trajectories and risk scores generated by NSTP-Net are expected to be translated into clinical decision support tools. With the integration of more data and biological knowledge, we hope that such models will eventually become the 'computational microscope' for neurologists, revealing individual specific disease dynamics through complex clinical manifestations, and promoting the diagnosis and treatment of neurodegenerative diseases into the era of precision medicine.

Future work will focus on the following directions:

1 External validation in a more diverse population cohort, such as AIBL, to evaluate the generalisation ability of the model.

2 Incorporate more cell type-specific mechanisms (e.g., microglia and astrocytes) to construct a more refined multi-cellular scale model.

3 Explore the introduction of a causal reasoning framework to further distinguish between correlational and causal relationships.

4 Optimise the computational efficiency and user interface, and promote the transformation of the model into a clinical practical tool.

Declarations

All authors declare that they have no conflicts of interest.

References

Arriagada, P.V., Growdon, J.H., Hedley-Whyte, E.T. and Hyman, B.T. (1992) 'Neurofibrillary tangles but not senile plaques parallel duration and severity of Alzheimer's disease', *Neurology*, Vol. 42, No. 3, pp.631–631.

Bhuyan, B.P., Ramdane-Cherif, A., Tomar, R. and Singh, T. (2024) 'Neuro-symbolic artificial intelligence: a survey', *Neural Computing and Applications*, Vol. 36, No. 21, pp.12809–12844.

Braak, H. and Braak, E. (1991) 'Neuropathological stageing of Alzheimer-related changes', *Acta Neuropathologica*, Vol. 82, No. 4, pp.239–259.

Chen, F., Wang, Y-C., Wang, B. and Kuo, C-C.J. (2020) 'Graph representation learning: a survey', *APSIPA Transactions on Signal and Information Processing*, Vol. 9, No. 1, p.e15.

De Strooper, B. and Karran, E. (2016) 'The cellular phase of Alzheimer's disease', *Cell*, Vol. 164, No. 4, pp.603–615.

Desikan, R.S., Ségonne, F., Fischl, B., Quinn, B.T., Dickerson, B.C., Blacker, D., Buckner, R.L., Dale, A.M., Maguire, R.P. and Hyman, B.T. (2006) 'An automated labeling system for subdividing the human cerebral cortex on MRI scans into gyral based regions of interest', *Neuroimage*, Vol. 31, No. 3, pp.968–980.

Garcez, A.d.A. and Lamb, L.C. (2023) 'Neurosymbolic AI: the 3rd wave', *Artificial Intelligence Review*, Vol. 56, No. 11, pp.12387–12406.

Hamet, P. and Tremblay, J. (2017) 'Artificial intelligence in medicine', *Metabolism*, Vol. 69, pp.S36–S40.

Huang, Q., Guo, X., Wang, Y., Sun, H. and Yang, L. (2024) 'A survey of feature matching methods', *IET Image Processing*, Vol. 18, No. 6, pp.1385–1410.

Islam, M., Islam, M.A. and Habib, A. (2023) 'Potato late blight disease detection using convolutional neural network', *International Journal of Information and Communication Technology*, Vol. 23, No. 4, pp.346–370.

Jellinger, K.A., Wenning, G.K. and Stefanova, N. (2021) 'Is multiple system atrophy a prion-like disorder?', *International Journal of Molecular Sciences*, Vol. 22, No. 18, p.10093.

Kumar, A. (2024) 'Neuro-Symbolic AI frameworks for explainable autonomous decision-making in complex environments', *International Journal of Advanced Research in Computer Science & Technology (IJARCST)*, Vol. 7, No. 6, pp.11345–11352.

Liang, B., Wang, Y. and Tong, C. (2025) 'AI reasoning in deep learning era: from symbolic AI to neural-symbolic AI', *Mathematics*, Vol. 13, No. 11, p.1707.

Liu, L., Drouet, V., Wu, J.W., Witter, M.P., Small, S.A., Clelland, C. and Duff, K. (2012) 'Trans-synaptic spread of tau pathology in vivo', *PloS One*, Vol. 7, No. 2, p.e31302.

Parisot, S., Ktena, S.I., Ferrante, E., Lee, M., Guerrero, R., Glocker, B. and Rueckert, D. (2018) 'Disease prediction using graph convolutional networks: application to autism spectrum disorder and Alzheimer's disease', *Medical Image Analysis*, Vol. 48, No. 1, pp.117–130.

Prusiner, S.B. (2013) 'Biology and genetics of prions causing neurodegeneration', *Annual Review of Genetics*, Vol. 47, No. 1, pp.601–623.

Raj, A., Kuceyeski, A. and Weiner, M. (2012) 'A network diffusion model of disease progression in dementia', *Neuron*, Vol. 73, No. 6, pp.1204–1215.

Schöll, M., Lockhart, S.N., Schonhaut, D.R., O'Neil, J.P., Janabi, M., Ossenkoppele, R., Baker, S.L., Vogel, J.W., Faria, J. and Schwimmer, H.D. (2016) 'PET imaging of tau deposition in the aging human brain', *Neuron*, Vol. 89, No. 5, pp.971–982.

Seixas, F., Conci, A., Muchaluat-Saade, D. and De Souza, A. (2009) 'Intelligent automated brain image segmentation', *International Journal of Innovative Computing and Applications*, Vol. 2, No. 1, pp.23–33.

Shukla, A. and Tiwari, R. (2008) 'A novel approach of speaker authentication by fusion of speech and image features using Artificial Neural Networks', *International Journal of Information and Communication Technology*, Vol. 1, No. 2, pp.159–170.

Sweller, J. (1988) 'Cognitive load during problem solving: effects on learning', *Cognitive science*, Vol. 12, No. 2, pp.257–285.

Therriault, J., Benedet, A.L., Pascoal, T.A., Mathotaarachchi, S., Chamoun, M., Savard, M., Thomas, E., Kang, M.S., Lussier, F. and Tissot, C. (2020) 'Association of apolipoprotein E ε4 with medial temporal tau independent of amyloid-β', *JAMA Neurology*, Vol. 77, No. 4, pp.470–479.

Tian, X., Liu, Y., Wang, L., Zeng, X., Huang, Y. and Wang, Z. (2023) 'An extensible hierarchical graph convolutional network for early Alzheimer's disease identification', *Computer Methods and Programs in Biomedicine*, Vol. 238, p.107597.

Yeh, C.H., Jones, D.K., Liang, X., Descoteaux, M. and Connelly, A. (2021) 'Mapping structural connectivity using diffusion MRI: challenges and opportunities', *Journal of Magnetic Resonance Imaging*, Vol. 53, No. 6, pp.1666–1682.

Zhou, J., Gennatas, E.D., Kramer, J.H., Miller, B.L. and Seeley, W.W. (2012) 'Predicting regional neurodegeneration from the healthy brain functional connectome', *Neuron*, Vol. 73, No. 6, pp.1216–1227.

Zhou, L., McInnes, J., Wierda, K., Holt, M., Herrmann, A.G., Jackson, R.J., Wang, Y-C., Swerts, J., Beyens, J. and Miskiewicz, K. (2017) 'Tau association with synaptic vesicles causes presynaptic dysfunction', *Nature Communications*, Vol. 8, No. 1, p.15295.